Eur. Phys. J. C (2014) 74:3077
DOI 10.1140/epjc/s10052-014-3077-y

THE EUROPEAN PHYSICAL JOURNAL C

Regular Article - Experimental Physics

Event-by-event mean p_{T} fluctuations in pp and Pb–Pb collisions at the LHC

ALICE Collaboration[*]

CERN, 1211 Geneva 23, Switzerland

Received: 22 July 2014 / Accepted: 12 September 2014 / Published online: 15 October 2014

Abstract Event-by-event fluctuations of the mean transverse momentum of charged particles produced in pp collisions at $\sqrt{s} = 0.9$, 2.76 and 7 TeV, and Pb–Pb collisions at $\sqrt{s_{\mathrm{NN}}} = 2.76$ TeV are studied as a function of the charged-particle multiplicity using the ALICE detector at the LHC. Dynamical fluctuations indicative of correlated particle emission are observed in all systems. The results in pp collisions show little dependence on collision energy. The Monte Carlo event generators PYTHIA and PHOJET are in qualitative agreement with the data. Peripheral Pb–Pb data exhibit a similar multiplicity dependence as that observed in pp. In central Pb–Pb, the results deviate from this trend, featuring a significant reduction of the fluctuation strength. The results in Pb–Pb are in qualitative agreement with previous measurements in Au–Au at lower collision energies and with expectations from models that incorporate collective phenomena.

1 Introduction

The study of event-by-event fluctuations was proposed as a probe of the properties of the hot and dense matter generated in high-energy heavy-ion collisions [1–9]. The occurrence of a phase transition from the Quark-Gluon Plasma to a Hadron Gas or the existence of a critical point in the phase diagram of strongly interacting matter may go along with critical fluctuations of thermodynamic quantities such as temperature. This could be reflected in dynamical event-by-event fluctuations of the mean transverse momentum $\left(\langle p_{\mathrm{T}}\rangle\right)$ of final-state charged particles.

Event-by-event $\langle p_{\mathrm{T}}\rangle$ fluctuations have been studied in nucleus-nucleus (A–A) collisions at the Super Proton Synchrotron (SPS) [10–14] and at the Relativistic Heavy-Ion Collider (RHIC) [15–20], where dynamical fluctuations have been observed. Fluctuations of $\langle p_{\mathrm{T}}\rangle$ were found to decrease with collision centrality, as generally expected in a dilution scenario caused by superposition of partially independent particle-emitting sources. In detail, however, deviations from a simple superposition scenario have been reported. In particular, with respect to a reference representing independent superposition – i.e. a decrease of fluctuations according to $\langle \mathrm{d}N_{\mathrm{ch}}/\mathrm{d}\eta\rangle^{-0.5}$, where $\langle \mathrm{d}N_{\mathrm{ch}}/\mathrm{d}\eta\rangle$ is the average charged-particle density in a given interval of collision centrality and pseudorapidity (η) – the observed fluctuations increase sharply from peripheral to semi-peripheral collisions, followed by a shallow decrease towards central collisions [18]. A number of possible mechanisms have been proposed to explain this behavior, such as string percolation [21] or the onset of thermalization and collectivity [22,23], but no strong connection to critical behavior could be made. It was recently suggested [24,25] that initial state density fluctuations [26] could affect the final state transverse momentum correlations and their centrality dependence.

Fluctuations of $\langle p_{\mathrm{T}}\rangle$ arise from many kinds of correlations among the p_{T} of the final-state particles, such as resonance decays, jets, or quantum correlations. To account for these contributions from conventional mechanisms similar studies can be performed in pp, where such correlations are also present. The results from pp could thus be used to construct a model-independent baseline to search for non-trivial fluctuations in A–A which manifest themselves in a modification of the fluctuation pattern with respect to the pp reference.

In this paper, we present results of a multiplicity-dependent study of event-by-event $\langle p_{\mathrm{T}}\rangle$ fluctuations of charged particles in pp collisions at $\sqrt{s} = 0.9$, 2.76 and 7 TeV, and Pb–Pb collisions at $\sqrt{s_{\mathrm{NN}}} = 2.76$ TeV measured with ALICE at the LHC. The experimental data are compared to different Monte Carlo (MC) event generators.

2 ALICE detector and data analysis

The data used in this analysis were collected with the ALICE detector at the CERN Large Hadron Collider (LHC) [27] during the Pb–Pb run in 2010 and the pp runs in 2010 and 2011.

[*] e-mail: alice-publications@cern.ch

For a detailed description of the ALICE apparatus see [28]. The analysis is based on 19×10^6 Pb–Pb events at $\sqrt{s_{\rm NN}} = 2.76$ TeV, and 6.9×10^6, 66×10^6 and 290×10^6 pp events at $\sqrt{s} = 0.9$, 2.76 and 7 TeV, respectively. The standard ALICE coordinate system is used, in which the nominal interaction point is the origin of a right-handed Cartesian coordinate system. The z-axis is along the beam pipe, the x-axis points towards the center of the LHC, φ is the azimuthal angle around the z-axis and θ is the polar angle with respect to this axis. The detectors in the central barrel of the experiment are operated inside a solenoidal magnetic field with $B = 0.5$ T. About half of the Pb–Pb data set was recorded with negative ($B_z < 0$) and positive ($B_z > 0$) field polarity, respectively.

A minimum bias (MB) trigger condition was applied to select collision events. In pp, this trigger was defined by at least one hit in the Silicon Pixel Detector (SPD) or in one of the two forward scintillator systems VZERO-A ($2.8 < \eta < 5.1$) and VZERO-C ($-3.7 < \eta < -1.7$). In Pb–Pb, the MB trigger condition is defined as a coincidence of hits in both VZERO detectors.

In this analysis, the Time Projection Chamber (TPC) [29] is used for charged-particle tracking in $|\eta| < 0.8$. In the momentum range selected for this analysis, $0.15 < p_{\rm T} < 2$ GeV/c, the momentum resolution $\sigma(p_{\rm T})/p_{\rm T}$ is better than 2 %. The tracking efficiency is larger than 90 % for $p_{\rm T} > 0.3$ GeV/c and drops to about 70 % at $p_{\rm T} = 0.15$ GeV/c.

Primary vertex information is obtained from both the Inner Tracking System (ITS) and the TPC. Events are used in the analysis when at least one accepted charged-particle track contributes to the primary vertex reconstruction. It is required that the reconstructed vertex is within ± 10 cm from the nominal interaction point along the beam direction to ensure a uniform pseudo-rapidity acceptance within the TPC. Additionally, the event vertex is reconstructed using only TPC tracks. The event is rejected if the z-position of that vertex is different by more than 10 cm from that of the standard procedure.

In Pb–Pb, at least 10 reconstructed tracks inside the acceptance are required. The contamination by non-hadronic interactions is negligible in the event sample that fulfills the aforementioned selection criteria. The centrality in Pb–Pb is estimated from the signal in the VZERO detectors using the procedure described in [30,31].

The charged-particle tracks used for this analysis are required to have at least 70 out of a maximum of 159 reconstructed space points in the TPC, and the maximum χ^2 per space point in the TPC from the momentum fit must be less than 4. Daughter tracks from reconstructed secondary weak-decay topologies (*kinks*) are rejected. The distance of closest approach (DCA) of the extrapolated trajectory to the primary vertex position is restricted to less than 3.2 cm along the beam direction and less than 2.4 cm in the transverse plane. The number of tracks in an event that are accepted by these selection criteria is denoted by $N_{\rm acc}$.

Event-by-event measurements of the mean transverse momentum are subject to the finite reconstruction efficiency of the detector. While efficiency corrections can be applied on a statistical basis to derive the inclusive $\langle p_{\rm T} \rangle$ of charged particles in a given kinematic acceptance range, such an approach is not adequate for event-by-event studies. The event-by-event mean transverse momentum is therefore approximated by the mean value $M_{\rm EbE}(p_{\rm T})_k$ of the transverse momenta $p_{{\rm T},i}$ of the $N_{{\rm acc},k}$ accepted charged particles in event k:

$$M_{\rm EbE}(p_{\rm T})_k = \frac{1}{N_{{\rm acc},k}} \sum_{i=1}^{N_{{\rm acc},k}} p_{{\rm T},i}. \tag{1}$$

Event-by-event fluctuations of $M_{\rm EbE}(p_{\rm T})_k$ in heavy-ion collisions are composed of statistical and dynamical contributions. The two-particle transverse momentum correlator $C = \langle \Delta p_{{\rm T},i}, \Delta p_{{\rm T},j} \rangle$ is a measure of the dynamical component $\sigma^2_{\rm dyn}$ of these fluctuations and therefore well suited for an event-by-event analysis [13,18,32]. The correlator C_m is the mean of covariances of all pairs of particles i and j in the same event with respect to the inclusive $M(p_{\rm T})_m$ in a given multiplicity class m and is defined as

$$C_m = \frac{1}{\sum_{k=1}^{n_{{\rm ev},m}} N_k^{\rm pairs}} \cdot \sum_{k=1}^{n_{{\rm ev},m}} \sum_{i=1}^{N_{{\rm acc},k}} \sum_{j=i+1}^{N_{{\rm acc},k}} (p_{{\rm T},i} - M(p_{\rm T})_m) \cdot (p_{{\rm T},j} - M(p_{\rm T})_m), \tag{2}$$

where $n_{{\rm ev},m}$ is the number of events in multiplicity class m, $N_k^{\rm pairs} = 0.5 \cdot N_{{\rm acc},k} \cdot (N_{{\rm acc},k} - 1)$ is the number of particle pairs in event k and $M(p_{\rm T})_m$ is the average $p_{\rm T}$ of all tracks in all events of class m:

$$M(p_{\rm T})_m = \frac{1}{\sum_{k=1}^{n_{{\rm ev},m}} N_{{\rm acc},k}} \sum_{k=1}^{n_{{\rm ev},m}} \sum_{i=1}^{N_{{\rm acc},k}} p_{{\rm T},i} = \frac{1}{\sum_{k=1}^{n_{{\rm ev},m}} N_{{\rm acc},k}} \sum_{k=1}^{n_{{\rm ev},m}} N_{{\rm acc},k} \cdot M_{\rm EbE}(p_{\rm T})_k. \tag{3}$$

By construction, C_m vanishes in the case of uncorrelated particle emission, when only statistical fluctuations are present.

The results in this paper are presented in terms of the dimensionless ratio $\sqrt{C_m}/M(p_{\rm T})_m$ which quantifies the strength of the dynamical fluctuations in units of the average transverse momentum $M(p_{\rm T})_m$ in the multiplicity class m.

The correlator is computed in intervals of the event multiplicity $N_{\rm acc}$. In pp collisions, intervals of $\Delta N_{\rm acc} = 1$ are used for the calculation of C_m and $M(p_{\rm T})_m$. In Pb–Pb collisions, C_m is calculated in the multiplicity intervals $\Delta N_{\rm acc} = 10$ for $N_{\rm acc} < 200$, $\Delta N_{\rm acc} = 25$ for $200 \leq N_{\rm acc} < 1000$ and

Table 1 Contributions to the total systematic uncertainty on $\sqrt{C_m}/M(p_T)_m$ in pp and Pb–Pb collisions. Ranges are given when the uncertainties depend on $\langle dN_{ch}/d\eta \rangle$ or centrality

Collision system $\sqrt{s_{NN}}$	pp 0.9 TeV	pp 2.76 TeV	pp 7 TeV	Pb–Pb 2.76 TeV
Vertex z-position cut	0–0.5 %	<0.1 %	<0.1 %	0.5–1 %
Vertex calculation	0–2 %	0.5–2 %	0.5–2 %	<0.1 %
Vertex difference cut	0–1.5 %	0–3 %	0–2 %	0–2 %
Min. TPC space points	1.5–3 %	1–2 %	1–3 %	2–3 %
TPC χ^2 / d.o.f.	<0.1 %	<0.1 %	<0.1 %	<0.1 %
DCA to vertex	1 %	1–1.5 %	0.5–1 %	0.5–1 %
B-field polarity	0.5 %	0.5 %	0.5 %	0.5 %
Centrality intervals	–	–	–	1–3 %
TPC-only vs. hybrid	4 %	4 %	4 %	1–5 %
MC generator vs. full sim.	0–6 %	0–6 %	0–6 %	0–4 %
Total	4.4–7.7 %	4.4–7.6 %	4.4–7.9 %	4.2–7.4 %

$\Delta N_{acc} = 100$ for $N_{acc} \geq 1000$. To account for the steep increase of $M(p_T)_m$ with multiplicity in peripheral collisions, the calculation of the correlator in (2) uses values for $M(p_T)_m$ which are calculated in bins of $\Delta N_{acc} = 1$ for $N_{acc} < 1000$. At higher multiplicities, $M(p_T)$ changes only moderately and $M(p_T)_m$ is calculated in the same intervals as C_m, i.e. $\Delta N_{acc} = 100$.

Additionally, the Pb–Pb data are also analyzed in 5 % intervals of the collision centrality. The results are shown in bins of the mean number of participating nucleons $\langle N_{part} \rangle$ as derived from the centrality percentile using a Glauber MC calculation [30]. For the results presented as a function of the mean charged-particle density $\langle dN_{ch}/d\eta \rangle$, the mean value $\langle N_{acc} \rangle$ in each centrality bin is associated with the measured value for $\langle dN_{ch}/d\eta \rangle$ from [30]. A linear relation between $\langle N_{acc} \rangle$ and $\langle dN_{ch}/d\eta \rangle$ is observed over the full centrality range, allowing interpolation to assign a value for $\langle dN_{ch}/d\eta \rangle$ to any interval of N_{acc}. In pp, $\langle dN_{ch}/d\eta \rangle$ is calculated for each interval of N_{acc} employing the full detector response matrix from MC and unfolding of the measured N_{acc} distributions following the procedure outlined in [33].

The systematic uncertainties are estimated separately for each collision system (Pb–Pb and pp) and at each collision energy. The relative uncertainties on $\sqrt{C_m}/M(p_T)_m$ are generally smaller than those on C_m because most of the sources of uncertainties lead to correlated variations of $M(p_T)_m$ and C_m that tend to cancel in the ratio $\sqrt{C_m}/M(p_T)_m$. Therefore, all quantitative results shown below are presented in terms of $\sqrt{C_m}/M(p_T)_m$. The contributions to the total systematic uncertainty on $\sqrt{C_m}/M(p_T)_m$ in pp and Pb–Pb collisions are summarized in Table 1. Ranges are given when the uncertainties depend on $\langle dN_{ch}/d\eta \rangle$ or centrality.

The largest contribution to the total systematic uncertainty results from the comparison of $\sqrt{C_m}/M(p_T)_m$ from full MC simulations employing a GEANT3 [34] implementation of the ALICE detector setup [35] to the MC generator level. Processing the events through the full simulation chain alters the result for $\sqrt{C_m}/M(p_T)_m$ with respect to the MC generator level by up to 6 % in high multiplicity pp collisions. This includes effects of tracking efficiency dependence on the transverse momentum. The studies in pp are performed using the Perugia-0 tune of PYTHIA6 [36,37], similar results are obtained with PHOJET [38]. HIJING [39] is used for Pb–Pb collisions, where the differences are slightly smaller, reaching up to 4 % in most central collisions.

Since these deviations are in general dependent on the event characteristics assumed in the model, in particular on the nature of the underlying particle correlations, no correction of experimental results is performed. Instead, these deviations are added to the systematic data uncertainties to allow for a comparison of the experimental results to model calculations on the MC event generator level.

Another major contribution to the total systematic uncertainty emerges from the difference between the standard analysis using only TPC tracks and an alternative analysis employing a hybrid tracking scheme. The hybrid tracking combines TPC and ITS tracks when ITS detector information is available, and thus provides more powerful suppression of secondary particles (remaining contamination 4–5 %) as compared to the standard TPC-only tracking (∼12 %). The TPC, on the other hand, features very stable operational conditions throughout the analyzed data sets. The differences between the results from the two analyses reach 5 % in $\sqrt{C_m}/M(p_T)_m$.

At the event level, minor contributions to the total systematic uncertainty arise from the cut on the maximum distance of the reconstructed vertex to the nominal interaction point along the beam axis. In the standard analysis global tracks that combine TPC and ITS track segments are used for the vertex calculation. Alternatively, we studied also the results when only TPC tracks or only tracklets from the SPD are used to reconstruct the primary vertex. The effect from

using the different vertex estimators is negligible in Pb–Pb collisions. In pp collisions, this effect is small with the exception of the lowest multiplicity bin, where it reaches 2 % in $\sqrt{C_m}/M(p_T)_m$. Additionally, the cut on the difference between the z-positions of the reconstructed vertices obtained from global tracks and TPC-only tracks is varied. This shows a sizable effect only in peripheral Pb–Pb and low-multiplicity pp collisions (2–3 % in $\sqrt{C_m}/M(p_T)_m$).

In addition, variations of the following track quality cuts are performed: the number of space points per track in the TPC, the χ^2 per degree of freedom of the momentum fit, and the DCA of each track to the primary vertex, both along the beam direction and in the transverse plane. Neither of these contributions to the total systematic uncertainty exceeds 3 % in $\sqrt{C_m}/M(p_T)_m$.

The difference between the results obtained from Pb–Pb data taken at the two magnetic field polarities is included into the systematic uncertainties. The effect is small (0.5 % in $\sqrt{C_m}/M(p_T)_m$). The corresponding uncertainty in pp is assumed to be the same as in Pb–Pb collisions. Finally, the effect of finite centrality intervals in Pb–Pb, and the corresponding variation of $M(p_T)$ within these intervals, is taken into account by including the difference between the analyses in 5 and 10 % centrality intervals [30,31] into the systematic uncertainty. The total uncertainty on $\sqrt{C_m}/M(p_T)_m$ for each data set was obtained by adding in quadrature the individual contributions in Table 1.

3 Results in pp collisions

The relative dynamical fluctuation $\sqrt{C_m}/M(p_T)_m$ as a function of the average charged-particle multiplicity $\langle dN_{ch}/d\eta\rangle$ in pp collisions at $\sqrt{s} = 0.9$, 2.76 and 7 TeV is shown in Fig. 1. The non-zero values of $\sqrt{C_m}/M(p_T)_m$ indicate significant dynamical event-by-event $M(p_T)$ fluctuations. The fluctuation strength reaches a maximum of 12–14 % in low multiplicity collisions and decreases to about 5 % at the highest multiplicities. No significant beam energy dependence is observed for the relative fluctuation $\sqrt{C_m}/M(p_T)_m$.

The beam energy dependence of relative dynamical mean transverse momentum fluctuations in pp collisions was studied at lower collision energies by the Split Field Magnet (SFM) detector at the Intersection Storage Rings (ISR). The SFM experiment measured relative fluctuations in inclusive pp collisions at $\sqrt{s} = 30.8$, 45, 52, and 63 GeV [40]. The fluctuations are expressed by the quantity R that is extracted from the multiplicity dependence of the event-by-event $M(p_T)$ dispersion. The measure $R = [D(M_{EbE}(p_T)_k)/M(p_T)]_{n\to\infty}$ is obtained from an extrapolation of the multiplicity-dependent dispersion $D(M_{EbE}(p_T)_k)$ to infinite multiplicity, normalized by the inclusive mean transverse momentum. It is an alternative approach to extract dynamical transverse momentum fluctuations in inclusive pp collisions.

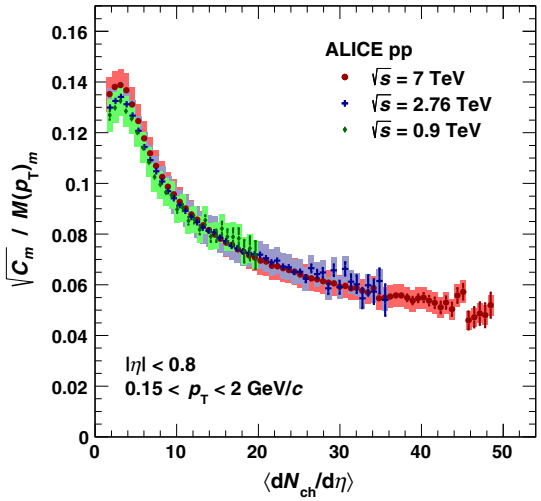

Fig. 1 Relative fluctuation $\sqrt{C_m}/M(p_T)_m$ as a function of $\langle dN_{ch}/d\eta\rangle$ in pp collisions at $\sqrt{s} = 0.9$, 2.76 and 7 TeV

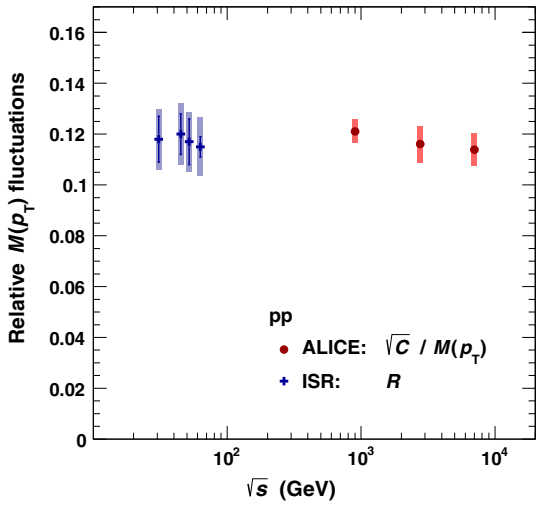

Fig. 2 Relative dynamical mean transverse momentum fluctuations in pp collisions as a function of $\sqrt{s}$. The ALICE results for $\sqrt{C}/M(p_T)$ are compared to the quantity R measured at the ISR (see text and [40])

To allow for a comparison to ISR results, an inclusive analysis of ALICE pp data is performed. The relative fluctuation $\sqrt{C}/M(p_T)$ is computed at each collision energy as in (2), however, without subdivision into multiplicity classes m. Monte Carlo studies of pp collisions at $\sqrt{s} = 7$ TeV using PYTHIA8 have shown that results for R and $\sqrt{C}/M(p_T)$ agree within 10–15 %. The ALICE results for the inclusive $\sqrt{C}/M(p_T)$ as a function of $\sqrt{s}$ are shown in Fig. 2, along with the ISR results for R from [40]. No significant dependence of the relative transverse momentum fluctuations on the collision energy is observed over this large energy range.

The results in pp at $\sqrt{s} = 7$ TeV are compared with results from different event generators. In particular, PYTHIA6

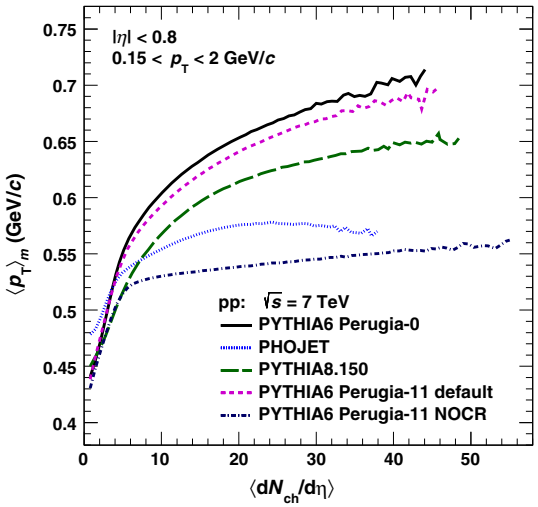

Fig. 3 Results for $\langle p_{\mathrm{T}}\rangle_m$ as a function of $\langle \mathrm{d}N_{\mathrm{ch}}/\mathrm{d}\eta\rangle$ in pp collisions at $\sqrt{s} = 7$ TeV from different event generators

(tunes Perugia-0 and Perugia-11), PYTHIA8.150 and PHOJET have been used.

It has been pointed out that high-multiplicity events in pp collisions at LHC energies are driven by multi-parton interactions (MPIs) [41]. This picture is also suggested by recent studies of the event sphericity in pp collisions [42]. MPIs are independent processes on the perturbative level. However, the color reconnection mechanism between produced strings may lead to correlations in the hadronic final state. Color reconnection is also the driving mechanism in PYTHIA for the increase of $\langle p_{\mathrm{T}}\rangle$ as a function of N_{ch} [43,44].

The default PYTHIA6 Perugia-11 tune including the color-reconnection mechanism is compared to results of the same tune without color-reconnection (NOCR). Figure 3 shows model calculations for $\langle p_{\mathrm{T}}\rangle_m$ as a function of $\langle \mathrm{d}N_{\mathrm{ch}}/\mathrm{d}\eta\rangle$ in $0.15 < p_{\mathrm{T}} < 2$ GeV/c and $|\eta| < 0.8$ in pp collisions at $\sqrt{s} = 7$ TeV. The MC generators yield qualitatively different results for the multiplicity dependence, in particular PHOJET and the NOCR version of PYTHIA6 Perugia-11 show only little increase of $\langle p_{\mathrm{T}}\rangle_m$ with multiplicity. Good agreement between PYTHIA8 and ALICE results in pp collisions at $\sqrt{s} = 7$ TeV was demonstrated [44], albeit in a different η and p_{T} interval.

Results for the relative dynamical fluctuation measure $\sqrt{C_m}/M(p_{\mathrm{T}})_m$ in pp at $\sqrt{s} = 7$ TeV are compared to model calculations in Fig. 4. The data exhibit a clear power-law dependence with $\langle \mathrm{d}N_{\mathrm{ch}}/\mathrm{d}\eta\rangle$ except for very small multiplicities. A power-law fit of $\sqrt{C_m}/M(p_{\mathrm{T}})_m \propto \langle \mathrm{d}N_{\mathrm{ch}}/\mathrm{d}\eta\rangle^b$ in the interval $5 < \langle \mathrm{d}N_{\mathrm{ch}}/\mathrm{d}\eta\rangle < 30$ yields $b = -0.431 \pm 0.001\,(\mathrm{stat.}) \pm 0.021\,(\mathrm{syst.})$. The deviation of the power-law index from $b = -0.5$ indicates that the observed multiplicity dependence of $M(p_{\mathrm{T}})$ fluctuations in pp does not follow a simple superposition scenario, contrary to what might be expected for independent MPIs. All PYTHIA tunes under study agree with this finding to the extent that they exhibit a similar power-law index as the data. This is also true for the NOCR calculation which excludes the color reconnection mechanism in its present implementation in PYTHIA as a dominant source of correlations beyond the independent superposition scenario.

4 Results in Pb–Pb collisions

Results for the relative dynamical fluctuation $\sqrt{C_m}/M(p_{\mathrm{T}})_m$ in Pb–Pb collisions at $\sqrt{s_{\mathrm{NN}}} = 2.76$ TeV as a function of $\langle \mathrm{d}N_{\mathrm{ch}}/\mathrm{d}\eta\rangle$ are shown in Fig. 5. As for pp collisions, significant dynamical fluctuations as well

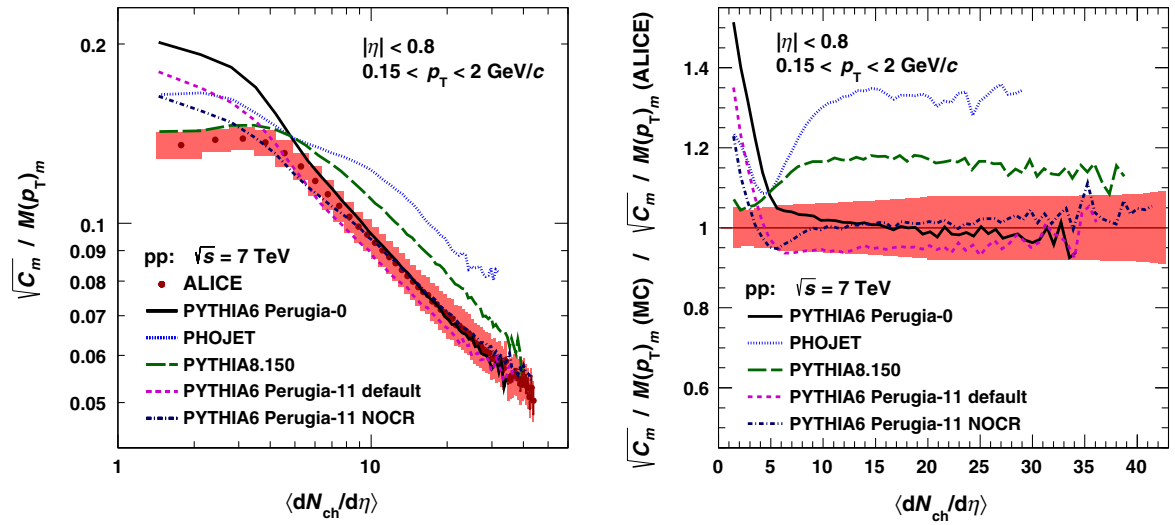

Fig. 4 *Left* Relative dynamical fluctuation $\sqrt{C_m}/M(p_{\mathrm{T}})_m$ for data and different event generators in pp collisions at $\sqrt{s} = 7$ TeV as a function of $\langle \mathrm{d}N_{\mathrm{ch}}/\mathrm{d}\eta\rangle$. *Right* Ratio models to data. The *red error band* indicates the statistical and systematic data uncertainties added in quadrature

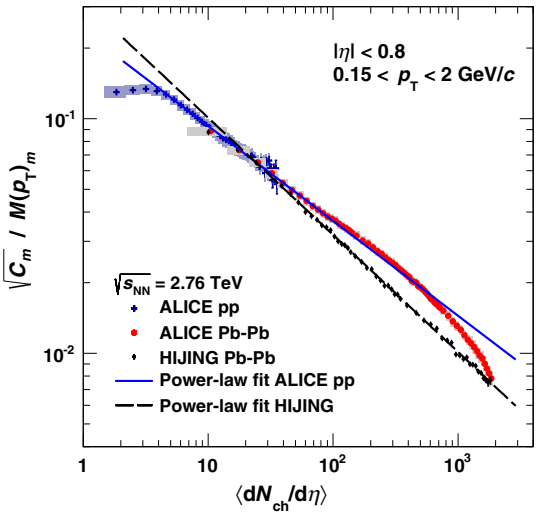

Fig. 5 Relative dynamical fluctuation $\sqrt{C_m}/M(p_T)_m$ as a function of $\langle dN_{ch}/d\eta\rangle$ in pp and Pb–Pb collisions at $\sqrt{s_{NN}} = 2.76$ TeV. Also shown are results from HIJING and power-law fits to pp (*solid line*) and HIJING (*dashed line*) (see text)

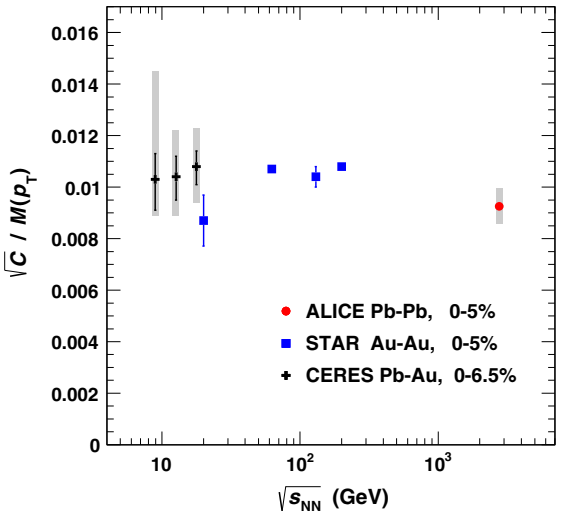

Fig. 6 Mean transverse momentum fluctuations in central heavy-ion collisions as a function of $\sqrt{s_{NN}}$. The ALICE data point is compared to data from the CERES [13] and STAR [18] experiments. For STAR only statistical uncertainties are available

as a strong decrease with multiplicity are observed. Also shown in Fig. 5 is the result of a HIJING [39] simulation (version 1.36) without jet-quenching. A power-law fit in the interval $30 < \langle dN_{ch}/d\eta\rangle < 1500$ describes the HIJING results very well, except at low multiplicities, and yields $b = -0.499 \pm 0.003\,(\text{stat.}) \pm 0.005\,(\text{syst.})$. The approximate $\langle dN_{ch}/d\eta\rangle^{-0.5}$ scaling reflects the basic property of HIJING as a superposition model of independent nucleon-nucleon collisions. The HIJING calculation, in particular the multiplicity dependence, is in obvious disagreement with the data.

In peripheral collisions $\left(\langle dN_{ch}/d\eta\rangle < 100\right)$, the Pb–Pb results are in very good agreement with the extrapolation of a power-law fit to pp data at $\sqrt{s} = 2.76$ TeV in the interval $5 < \langle dN_{ch}/d\eta\rangle < 25$, with $b = -0.405 \pm 0.002\,(\text{stat.}) \pm 0.036\,(\text{syst.})$. This is remarkable because significant differences in $\langle p_T\rangle$ are observed between pp and Pb–Pb in this multiplicity range [44]. At larger multiplicities, the Pb–Pb results deviate from the pp extrapolation. An enhancement in $100 < \langle dN_{ch}/d\eta\rangle < 500$ is followed by a pronounced decrease at $\langle dN_{ch}/d\eta\rangle > 500$, corresponding to centralities $< 40\,\%$, which indicates a strong reduction of fluctuations towards central collisions.

Measurements of mean transverse momentum fluctuations in central A–A collisions at the SPS [13] and at RHIC [18] are compared to the ALICE result in Fig. 6. As in pp, there is no significant dependence on $\sqrt{s_{NN}}$ observed over a wide range of collision energies.

Figure 7 shows a comparison of the ALICE results for $\sqrt{C_m}/M(p_T)_m$ to measurements in Au–Au collisions at $\sqrt{s_{NN}} = 200$ GeV by the STAR experiment at RHIC [18]. In the peripheral region, the STAR data show very similar scaling with $\langle dN_{ch}/d\eta\rangle$ as the ALICE data, as shown on the left panel of Fig. 7. Also shown are the fit to pp data at $\sqrt{s} = 2.76$ TeV from Fig. 5 and the result of a power-law fit to the STAR data in $\langle dN_{ch}/d\eta\rangle < 200$ where the power is fixed to $b = -0.405$. Good agreement of the ALICE and STAR data with the fits is observed in peripheral collisions. The decrease of fluctuations in central collisions is similar in ALICE and STAR, however, no significant enhancement in semi-central events is observed in the STAR data. In the right panel of Fig. 7, the results for $\sqrt{C_m}/M(p_T)_m$ in ALICE and STAR are shown as a function of the mean number of participating nucleons $\langle N_{part}\rangle$. In this representation, the measurements of $\sqrt{C_m}/M(p_T)_m$ from ALICE and STAR are compatible within the rather large experimental uncertainties on $\langle N_{part}\rangle$ in STAR. A power-law fit $\sqrt{C_m}/M(p_T)_m \propto \langle N_{part}\rangle^b$ to the ALICE data in the interval $10 < \langle N_{part}\rangle < 40$ yields $b = -0.472 \pm 0.007\,(\text{stat.}) \pm 0.037\,(\text{syst.})$. The agreement between ALICE and STAR data as a function of $\langle N_{part}\rangle$ points to a relation between the observed fluctuation patterns and the collision geometry.

Transverse momentum correlations and fluctuations may be modified as a consequence of collective flow in A–A collisions. It should be noted, however, that event-averaged radial flow and azimuthal asymmetries are not expected to give rise to strong transverse momentum fluctuations in azimuthally symmetric detectors [13,16]. On the other hand, $M(p_T)$ fluctuations may occur due to fluctuating initial conditions that are also related to event-by-event fluctuations of radial flow and azimuthal asymmetries. We compare our results to calculations from the AMPT model [45] which has been demonstrated to give a reasonable description of inclusive and event-averaged bulk properties in Pb–Pb collisions at LHC ener-

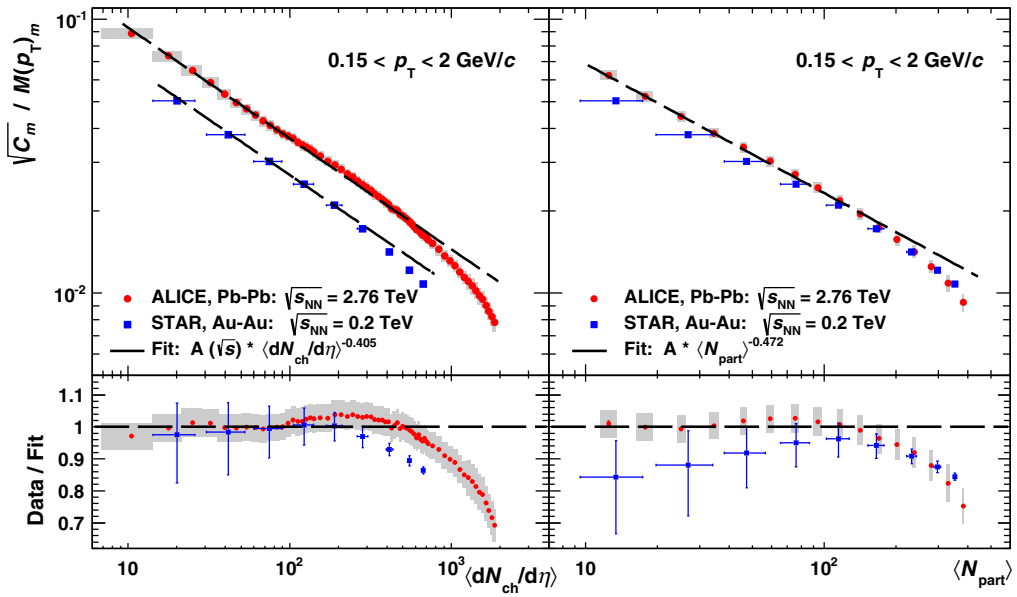

Fig. 7 *Left* Relative dynamical fluctuation $\sqrt{C_m}/M(p_T)_m$ as a function of $\langle dN_{ch}/d\eta \rangle$ in Pb–Pb collisions at $\sqrt{s_{NN}} = 2.76$ TeV from ALICE compared to results from STAR in Au–Au collisions at $\sqrt{s_{NN}} = 200$ GeV [18]. Also shown as *dashed lines* are results from power-law fits to the data (see text). *Right* same data as a function of $\langle N_{part} \rangle$

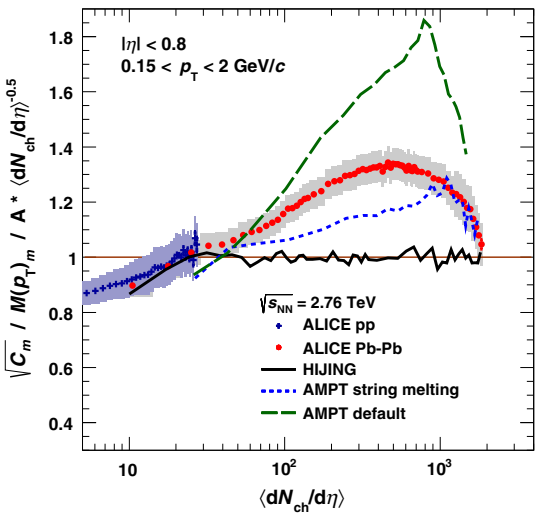

Fig. 8 Relative dynamical fluctuation $\sqrt{C_m}/M(p_T)_m$ normalized to $\langle dN_{ch}/d\eta \rangle^{-0.5}$ (see text) as a function of $\langle dN_{ch}/d\eta \rangle$ in pp and Pb–Pb collisions at $\sqrt{s_{NN}} = 2.76$ TeV. The ALICE data are compared to results from HIJING and AMPT

gies [46,47], in particular of the measured elliptic flow coefficient v_2. Figure 8 shows the ratio of $\sqrt{C_m}/M(p_T)_m$ in data and models to the result of a fit of $A \cdot \langle dN_{ch}/d\eta \rangle^{-0.5}$ to the HIJING simulation in the interval $30 < \langle dN_{ch}/d\eta \rangle < 1500$. For $\langle dN_{ch}/d\eta \rangle < 30$, HIJING agrees well with the results from pp and Pb–Pb. At larger multiplicities, none of the models shows quantitative agreement with the Pb–Pb data. The default AMPT calculation gives rise to increased fluctuations on top of the underlying HIJING scenario exceeding those observed in the data, except for very peripheral collisions. In contrast, the AMPT calculation with string melting, where partons after rescattering are recombined by a hadronic coalescence scheme, predicts smaller fluctuations. On the other hand, both AMPT versions exhibit a pronounced fall-off in central collisions which is in qualitative agreement with the data.

In a recent approach [24], initial spatial fluctuations of glasma flux tubes have been related to mean transverse momentum fluctuations of final state hadrons via their coupling to a collective flow field. A comparison of these calculations to data from ALICE and STAR is shown in [24]. Good agreement is found in the semi-central and central region, where the data deviate from the pp extrapolation.

5 Summary and conclusions

First results on event-by-event fluctuations of the mean transverse momentum of charged particles in pp and Pb–Pb collisions at the LHC are presented. Expressed in terms of the relative dynamical fluctuation $\sqrt{C_m}/M(p_T)_m$, little energy dependence of the mean transverse momentum fluctuations is observed in pp at $\sqrt{s} = 0.9$, 2.76 and 7 TeV. The results are also compatible with similar measurements at the ISR. For the first time, mean transverse momentum fluctuations in pp are studied as a function of $\langle dN_{ch}/d\eta \rangle$. A characteristic decrease of $\sqrt{C_m}/M(p_T)_m$ following a power law is observed. The decrease is weaker than expected from a superposition of independent sources. The nature of such sources in pp is subject to future studies, but a connection to the con-

cept of multi-parton interactions is suggestive. Model studies using PYTHIA however indicate that there is no strong sensitivity of transverse momentum fluctuations to the mechanism of color reconnection.

In peripheral Pb–Pb collisions $\left(\langle \mathrm{d}N_{\mathrm{ch}}/\mathrm{d}\eta\rangle < 100\right)$, the dependence of $\sqrt{C_m}/M(p_{\mathrm{T}})_m$ on $\langle \mathrm{d}N_{\mathrm{ch}}/\mathrm{d}\eta\rangle$ is very similar to that observed in pp collisions at the corresponding collision energy. At larger multiplicities, the Pb–Pb data deviate significantly from an extrapolation of pp results and show a strong decrease for $\langle \mathrm{d}N_{\mathrm{ch}}/\mathrm{d}\eta\rangle > 500$. The results for the most central collisions are of the same magnitude as previous measurements at the SPS and at RHIC. The centrality dependence of $\sqrt{C_m}/M(p_{\mathrm{T}})_m$ is compatible with that observed in Au–Au at $\sqrt{s_{\mathrm{NN}}} = 200$ GeV.

The Pb–Pb data can not be described by models based on independent nucleon-nucleon collisions such as HIJING. Models which include initial state density fluctuations and their effect on the development of collectivity in the final state are in qualitative agreement with the data. This suggests a connection between the observed fluctuations of transverse momentum and azimuthal correlations, and their relation to fluctuations in the initial state of the collision.

Acknowledgments The ALICE Collaboration would like to thank all its engineers and technicians for their invaluable contributions to the construction of the experiment and the CERN accelerator teams for the outstanding performance of the LHC complex. The ALICE Collaboration gratefully acknowledges the resources and support provided by all Grid centres and the Worldwide LHC Computing Grid (WLCG) collaboration. The ALICE Collaboration acknowledges the following funding agencies for their support in building and running the ALICE detector: State Committee of Science, World Federation of Scientists (WFS) and Swiss Fonds Kidagan, Armenia, Conselho Nacional de Desenvolvimento Científico e Tecnológico (CNPq), Financiadora de Estudos e Projetos (FINEP), Fundação de Amparo à Pesquisa do Estado de São Paulo (FAPESP); National Natural Science Foundation of China (NSFC), the Chinese Ministry of Education (CMOE) and the Ministry of Science and Technology of China (MSTC); Ministry of Education and Youth of the Czech Republic; Danish Natural Science Research Council, the Carlsberg Foundation and the Danish National Research Foundation; The European Research Council under the European Community's Seventh Framework Programme; Helsinki Institute of Physics and the Academy of Finland; French CNRS-IN2P3, the 'Region Pays de Loire', 'Region Alsace', 'Region Auvergne' and CEA, France; German BMBF and the Helmholtz Association; General Secretariat for Research and Technology, Ministry of Development, Greece; Hungarian OTKA and National Office for Research and Technology (NKTH); Department of Atomic Energy and Department of Science and Technology of the Government of India; Istituto Nazionale di Fisica Nucleare (INFN) and Centro Fermi - Museo Storico della Fisica e Centro Studi e Ricerche "Enrico Fermi", Italy; MEXT Grant-in-Aid for Specially Promoted Research, Japan; Joint Institute for Nuclear Research, Dubna; National Research Foundation of Korea (NRF); CONACYT, DGAPA, México, ALFA-EC and the EPLANET Program (European Particle Physics Latin American Network) Stichting voor Fundamenteel Onderzoek der Materie (FOM) and the Nederlandse Organisatie voor Wetenschappelijk Onderzoek (NWO), Netherlands; Research Council of Norway (NFR); Polish Ministry of Science and Higher Education; National Science Centre, Poland; Ministry of National Education/Institute for Atomic Physics and CNCS-UEFISCDI-Romania; Ministry of Education and Science of Russian Federation, Russian Academy of Sciences, Russian Federal Agency of Atomic Energy, Russian Federal Agency for Science and Innovations and The Russian Foundation for Basic Research; Ministry of Education of Slovakia; Department of Science and Technology, South Africa; CIEMAT, EELA, Ministerio de Economía y Competitividad (MINECO) of Spain, Xunta de Galicia (Consellería de Educación), CEADEN, Cubaenergía, Cuba, and IAEA (International Atomic Energy Agency); Swedish Research Council (VR) and Knut & Alice Wallenberg Foundation (KAW); Ukraine Ministry of Education and Science; United Kingdom Science and Technology Facilities Council (STFC); The United States Department of Energy, the United States National Science Foundation, the State of Texas, and the State of Ohio; Ministry of Science, Education and Sports of Croatia and Unity through Knowledge Fund, Croatia.

References

1. S. Jeon, V. Koch, Event by event fluctuations. arXiv:hep-ph/0304012 [hep-ph]
2. S. Mrowczynski, Plasma instability at the initial stage of ultrarelativistic heavy ion collisions. Phys. Lett. B **314**, 118–121 (1993)
3. L. Stodolsky, Temperature fluctuations in multiparticle production. Phys. Rev. Lett. **75**, 1044–1045 (1995)
4. E.V. Shuryak, Event per event analysis of heavy ion collisions and thermodynamical fluctuations. Phys. Lett. B **423**, 9–14 (1998). arXiv:hep-ph/9704456 [hep-ph]
5. M.A. Stephanov, K. Rajagopal, E.V. Shuryak, Signatures of the tricritical point in QCD. Phys. Rev. Lett. **81**, 4816–4819 (1998). arXiv:hep-ph/9806219 [hep-ph]
6. M.A. Stephanov, K. Rajagopal, E.V. Shuryak, Event-by-event fluctuations in heavy ion collisions and the QCD critical point. Phys. Rev. D **60**, 114028 (1999). arXiv:hep-ph/9903292 [hep-ph]
7. H. Heiselberg, Event-by-event physics in relativistic heavy ion collisions. Phys. Rept. **351**, 161–194 (2001). arXiv:nucl-th/0003046 [nucl-th]
8. A. Dumitru, R.D. Pisarski, Event-by-event fluctuations from decay of a Polyakov loop condensate. Phys. Lett. B **504**, 282–290 (2001). arXiv:hep-ph/0010083 [hep-ph]
9. Z. Fodor, S. Katz, Critical point of QCD at finite T and mu, lattice results for physical quark masses. JHEP **0404**, 050 (2004). arXiv:hep-lat/0402006 [hep-lat]
10. NA49 Collaboration, H. Appelshäuser et al., Event-by-event fluctuations of average transverse momentum in central Pb + Pb collisions at 158 GeV per nucleon, Phys. Lett. B **459**, 679–686 (1999). arXiv:hep-ex/9904014 [hep-ex]
11. CERES Collaboration, D. Adamová et al., Event by event fluctuations of the mean transverse momentum in 40, 80 and 158 A GeV / c Pb–Au collisions, Nucl. Phys. A **727**, 97–119 (2003). arXiv:nucl-ex/0305002 [nucl-ex]
12. NA49 Collaboration, T. Anticic et al., Transverse momentum fluctuations in nuclear collisions at 158-A GeV. Phys. Rev. **C70**, 034902 (2004). arXiv:hep-ex/0311009 [hep-ex]
13. CERES Collaboration, D. Adamová et al., Scale-dependence of transverse momentum correlations in Pb-Au collisions at 158A GeV/c, Nucl. Phys. A **811**, 179–196 (2008). arXiv:0803.2407 [nucl-ex].

14. NA49 Collaboration, T. Anticic et al., Energy dependence of transverse momentum fluctuations in Pb+Pb collisions at the CERN Super Proton Synchrotron (SPS) at 20A to 158A GeV. Phys. Rev. **C79**, 044904 (2009). arXiv:0810.5580 [nucl-ex]
15. PHENIX Collaboration, K. Adcox et al., Event-by-event fluctuations in mean p(T) and mean e(T) in $\sqrt{s_{NN}}$ = 130 GeV Au+Au collisions, Phys. Rev. C **66**, 024901 (2002). arXiv:nucl-ex/0203015 [nucl-ex]
16. PHENIX Collaboration, S. Adler et al., Measurement of nonrandom event by event fluctuations of average transverse momentum in $\sqrt{s_{NN}}$ = 200 GeV Au+Au and p+p collisions, Phys. Rev. Lett. **93** 092301 (2004). arXiv:nucl-ex/0310005 [nucl-ex]
17. STAR Collaboration, J. Adams et al., Event by event mean-p(t) fluctuations in Au-Au collisions at $\sqrt{s_{NN}}$ = 130 GeV, Phys. Rev. C **71** 064906 (2005). arXiv:nucl-ex/0308033 [nucl-ex]
18. STAR Collaboration, J. Adams et al., Incident energy dependence of pt correlations at RHIC, Phys. Rev. C **72**, 044902 (2005). arXiv:nucl-ex/0504031 [nucl-ex]
19. STAR Collaboration, J. Adams et al., Transverse-momentum p(t) correlations on (eta, phi) from mean-p(t) fluctuations in Au-Au collisions at $\sqrt{s_{NN}}$ = 200 GeV, J. Phys. G **32**, L37–L48 (2006). arXiv:nucl-ex/0509030 [nucl-ex]
20. STAR Collaboration, J. Adams et al., The Energy dependence of p_t angular correlations inferred from mean-p(t) fluctuation scale dependence in heavy ion collisions at the SPS and RHIC, J. Phys. G **34**, 451–466 (2007). arXiv:nucl-ex/0605021 [nucl-ex]
21. E. Ferreiro, F. del Moral, C. Pajares, Transverse momentum fluctuations and percolation of strings. Phys. Rev. C **69**, 034901 (2004). arXiv:hep-ph/0303137 [hep-ph]
22. S.A. Voloshin, Transverse radial expansion in nuclear collisions and two particle correlations, Phys. Lett. B **632**, 490–494 (2006). arXiv:nucl-th/0312065 [nucl-th]
23. S. Gavin, Traces of Thermalization from p_t Fluctuations in Nuclear Collisions. Phys. Rev. Lett. **92**, 162301 (2004). arXiv:nucl-th/0308067 [nucl-th]
24. S. Gavin, G. Moschelli, Fluctuation probes of early-time correlations in nuclear collisions. Phys. Rev. C **85**, 014905 (2012). arXiv:1107.3317 [nucl-th]
25. S. Gavin, G. Moschelli, Flow Fluctuations from Early-Time Correlations in Nuclear Collisions. Phys. Rev. **C86**, 034902 (2012). arXiv:1205.1218 [nucl-th]
26. B. Alver, G. Roland, Collision geometry fluctuations and triangular flow in heavy-ion collisions. Phys. Rev. C **81**, 054905 (2010). arXiv:1003.0194 [nucl-th]. Erratum: Phys. Rev. C **82**, 039903 (2010)
27. L. Evans, P. Bryant, LHC machine. JINST **3**, S08001 (2008)
28. ALICE Collaboration, K. Aamodt et al., The ALICE experiment at the CERN LHC, JINST **3**, S08002 (2008)
29. J. Alme et al., The ALICE TPC, a large 3-dimensional tracking device with fast readout for ultra-high multiplicity events. Nucl. Instrum. Meth. A **622**, 316–367 (2010). arXiv:1001.1950 [physics.ins-det]
30. ALICE Collaboration, K. Aamodt et al., Centrality dependence of the charged-particle multiplicity density at mid-rapidity in Pb-Pb collisions at $\sqrt{s_{NN}}$ = 2.76 TeV, Phys. Rev. Lett. **106**, 032301 (2011). arXiv:1012.1657 [nucl-ex]
31. ALICE Collaboration, B. Abelev et al., Centrality determination of Pb-Pb collisions at $\sqrt{s_{NN}}$ = 2.76 TeV with ALICE, Phys. Rev. C **88**(4), 044909 (2013). arXiv:1301.4361 [nucl-ex]
32. S. Voloshin, V. Koch, H. Ritter, Event-by-event fluctuations in collective quantities. Phys. Rev. C **60**, 024901 (1999). arXiv:nucl-th/9903060 [nucl-th]
33. ALICE Collaboration, K. Aamodt et al., Charged-particle multiplicity measurement in proton-proton collisions at $\sqrt{s}$ = 0.9 and 2.36 TeV with ALICE at LHC, Eur. Phys. J. C **68**, 89–108 (2010). arXiv:1004.3034 [hep-ex]
34. R. Brun, F. Carminati, S. Giani, GEANT Detector Description and Simulation Tool, CERN-W5013 (1994)
35. R. Brun, P. Buncic, F. Carminati, A. Morsch, F. Rademakers et al., Computing in ALICE. Nucl. Instrum. Meth. A **502**, 339–346 (2003)
36. T. Sjostrand, S. Mrenna, P.Z. Skands, PYTHIA 6.4 Physics and Manual, JHEP **05**, 026 (2006). arXiv:hep-ph/0603175 [hep-ph]
37. P.Z. Skands, Tuning Monte Carlo Generators: The Perugia Tunes. Phys. Rev. **D82**, 074018 (2010). arXiv:1005.3457 [hep-ph]
38. R. Engel, J. Ranft, S. Roesler, Hard diffraction in hadron hadron interactions and in photoproduction, Phys. Rev. D **52**, 1459–1468 (1995). arXiv:hep-ph/9502319 [hep-ph]
39. W.-T. Deng, X.-N. Wang, R. Xu, Gluon shadowing and hadron production in heavy-ion collisions at LHC, Phys. Lett. B **701**, 133–136 (2011). arXiv:1011.5907 [nucl-th]
40. CERN-Dortmund-Heidelberg-Warsaw-Ames-Bologna, CERN-Heidelberg-Lund Collaboration, K. Braune et al., Fluctuations in the Hadronic Temperature in pp, pα and $\alpha\alpha$ Collisions at ISR Energies, Phys. Lett. B **123** 467 (1983)
41. P. Bartalini, E. Berger, B. Blok, G. Calucci, R. Corke, et al., Multi-parton interactions at the LHC. arXiv:1111.0469 [hep-ph]
42. ALICE Collaboration, B. Abelev et al., Transverse sphericity of primary charged particles in minimum bias proton-proton collisions at $\sqrt{s}$ = 0.9, 2.76 and 7 TeV, Eur. Phys. J. C **72** 2124 (2012). arXiv:1205.3963 [hep-ex]
43. T. Sjostrand, Colour reconnection and its effects on precise measurements at the LHC. arXiv:1310.8073 [hep-ph]
44. ALICE Collaboration, B. Abelev et al., Multiplicity dependence of the average transverse momentum in pp, p-Pb, and Pb-Pb collisions at the LHC. Phys. Lett. B **727**, 371–380 (2013). arXiv:1307.1094 [nucl-ex]
45. Z.-W. Lin, C.M. Ko, B.-A. Li, B. Zhang, S. Pal, Multiphase transport model for relativistic heavy ion collisions. Phys. Rev. C **72**, 064901 (2005). arXiv:nucl-th/0411110 [nucl-th]
46. J. Xu, C.M. Ko, Triangular flow in heavy ion collisions in a multiphase transport model. Phys. Rev. C **84**, 014903 (2011). arXiv:1103.5187 [nucl-th]
47. J. Xu, C.M. Ko, Higher-order anisotropic flows and dihadron correlations in Pb-Pb collisions at $\sqrt{s_{NN}}$ = 2.76 TeV in a multiphase transport model. Phys. Rev. C **84**, 044907 (2011). arXiv:1108.0717 [nucl-th]

ALICE Collaboration

B. Abelev[71], J. Adam[37], D. Adamová[79], M. M. Aggarwal[83], G. Aglieri Rinella[34], M. Agnello[90,107], A. Agostinelli[26], N. Agrawal[44], Z. Ahammed[126], N. Ahmad[18], I. Ahmed[15], S. U. Ahn[64], S. A. Ahn[64], I. Aimo[90,107], S. Aiola[131], M. Ajaz[15], A. Akindinov[54], S. N. Alam[126], D. Aleksandrov[96], B. Alessandro[107], D. Alexandre[98], A. Alici[12,101], A. Alkin[3], J. Alme[35], T. Alt[39], S. Altinpinar[17], I. Altsybeev[125], C. Alves Garcia Prado[115], C. Andrei[74], A. Andronic[93], V. Anguelov[89], J. Anielski[50], T. Antičić[94], F. Antinori[104], P. Antonioli[101], L. Aphecetche[109], H. Appelshäuser[49], S. Arcelli[26], N. Armesto[16], R. Arnaldi[107], T. Aronsson[131], I. C. Arsene[21,93], M. Arslandok[49], A. Augustinus[34], R. Averbeck[93], T. C. Awes[80], M. D. Azmi[18,85], M. Bach[39], A. Badalà[103], Y. W. Baek[40,66], S. Bagnasco[107], R. Bailhache[49], R. Bala[86], A. Baldisseri[14], F. Baltasar Dos Santos Pedrosa[34], R. C. Baral[57], R. Barbera[27], F. Barile[31], G. G. Barnaföldi[130], L. S. Barnby[98], V. Barret[66], J. Bartke[112], M. Basile[26], N. Bastid[66], S. Basu[126], B. Bathen[50], G. Batigne[109], A. Batista Camejo[66], B. Batyunya[62], P. C. Batzing[21], C. Baumann[49], I. G. Bearden[76], H. Beck[49], C. Bedda[90], N. K. Behera[44], I. Belikov[51], F. Bellini[26], R. Bellwied[117], E. Belmont-Moreno[60], R. Belmont III[129], V. Belyaev[72], G. Bencedi[130], S. Beole[25], I. Berceanu[74], A. Bercuci[74], Y. Berdnikov[81,b], D. Berenyi[130], M. E. Berger[88], R. A. Bertens[53], D. Berzano[25], L. Betev[34], A. Bhasin[86], I. R. Bhat[86], A. K. Bhati[83], B. Bhattacharjee[41], J. Bhom[122], L. Bianchi[25], N. Bianchi[68], C. Bianchin[53], J. Bielčík[37], J. Bielčíková[79], A. Bilandzic[76], S. Bjelogrlic[53], F. Blanco[10], D. Blau[96], C. Blume[49], F. Bock[70,89], A. Bogdanov[72], H. Bøggild[76], M. Bogolyubsky[108], F. V. Böhmer[88], L. Boldizsár[130], M. Bombara[38], J. Book[49], H. Borel[14], A. Borissov[92,129], M. Borri[78], F. Bossú[61], M. Botje[77], E. Botta[25], S. Böttger[48], P. Braun-Munzinger[93], M. Bregant[115], T. Breitner[48], T. A. Broker[49], T. A. Browning[91], M. Broz[37], E. Bruna[107], G. E. Bruno[31], D. Budnikov[95], H. Buesching[49], S. Bufalino[107], P. Buncic[34], O. Busch[89], Z. Buthelezi[61], D. Caffarri[28,34], X. Cai[7], H. Caines[131], L. Calero Diaz[68], A. Caliva[53], E. Calvo Villar[99], P. Camerini[24], F. Carena[34], W. Carena[34], J. Castillo Castellanos[14], E. A. R. Casula[23], V. Catanescu[74], C. Cavicchioli[34], C. Ceballos Sanchez[9], J. Cepila[37], P. Cerello[107], B. Chang[118], S. Chapeland[34], J. L. Charvet[14], S. Chattopadhyay[126], S. Chattopadhyay[97], V. Chelnokov[3], M. Cherney[82], C. Cheshkov[124], B. Cheynis[124], V. Chibante Barroso[34], D. D. Chinellato[116,117], P. Chochula[34], M. Chojnacki[76], S. Choudhury[126], P. Christakoglou[77], C. H. Christensen[76], P. Christiansen[32], T. Chujo[122], S. U. Chung[92], C. Cicalo[102], L. Cifarelli[12,26], F. Cindolo[101], J. Cleymans[85], F. Colamaria[31], D. Colella[31], A. Collu[23], M. Colocci[26], G. Conesa Balbastre[67], Z. Conesa del Valle[47], M. E. Connors[131], J. G. Contreras[11,37], T. M. Cormier[80,129], Y. Corrales Morales[25], P. Cortese[30], I. Cortés Maldonado[2], M. R. Cosentino[115], F. Costa[34], P. Crochet[66], R. Cruz Albino[11], E. Cuautle[59], L. Cunqueiro[34,68], A. Dainese[104], R. Dang[7], A. Danu[58], D. Das[97], I. Das[47], K. Das[97], S. Das[4], A. Dash[116], S. Dash[44], S. De[126], H. Delagrange[109,a], A. Deloff[73], E. Dénes[130], G. D'Erasmo[31], A. De Caro[12,29], G. de Cataldo[100], J. de Cuveland[39], A. De Falco[23], D. De Gruttola[12,29], N. De Marco[107], S. De Pasquale[29], R. de Rooij[53], M. A. Diaz Corchero[10], T. Dietel[50,85], P. Dillenseger[49], R. Divià[34], D. Di Bari[31], S. Di Liberto[105], A. Di Mauro[34], P. Di Nezza[68], Ø. Djuvsland[17], A. Dobrin[53], T. Dobrowolski[73], D. Domenicis Gimenez[115], B. Dönigus[49], O. Dordic[21], S. Dørheim[88], A. K. Dubey[126], A. Dubla[53], L. Ducroux[124], P. Dupieux[66], A. K. Dutta Majumdar[97], T. E. Hilden[42], R. J. Ehlers[131], D. Elia[100], H. Engel[48], B. Erazmus[34,109], H. A. Erdal[35], D. Eschweiler[39], B. Espagnon[47], M. Esposito[34], M. Estienne[109], S. Esumi[122], D. Evans[98], S. Evdokimov[108], D. Fabris[104], J. Faivre[67], D. Falchieri[26], A. Fantoni[68], M. Fasel[70,89], D. Fehlker[17], L. Feldkamp[50], D. Felea[58], A. Feliciello[107], G. Feofilov[125], J. Ferencei[79], A. Fernández Téllez[2], E. G. Ferreiro[16], A. Ferretti[25], A. Festanti[28], J. Figiel[112], M. A. S. Figueredo[119], S. Filchagin[95], D. Finogeev[52], F. M. Fionda[31], E. M. Fiore[31], E. Floratos[84], M. Floris[34], S. Foertsch[61], P. Foka[93], S. Fokin[96], E. Fragiacomo[106], A. Francescon[28,34], U. Frankenfeld[93], U. Fuchs[34], C. Furget[67], A. Furs[52], M. Fusco Girard[29], J. J. Gaardhøje[76], M. Gagliardi[25], A. M. Gago[99], M. Gallio[25], D. R. Gangadharan[19,70], P. Ganoti[80,84], C. Gao[7], C. Garabatos[93], E. Garcia-Solis[13], C. Gargiulo[34], I. Garishvili[71], J. Gerhard[39], M. Germain[109], A. Gheata[34], M. Gheata[34,58], B. Ghidini[31], P. Ghosh[126], S. K. Ghosh[4], P. Gianotti[68], P. Giubellino[34], E. Gladysz-Dziadus[112], P. Glässel[89], A. Gomez Ramirez[48], P. González-Zamora[10], S. Gorbunov[39], L. Görlich[112], S. Gotovac[111], L. K. Graczykowski[128], A. Grelli[53], A. Grigoras[34], C. Grigoras[34], V. Grigoriev[72], A. Grigoryan[1], S. Grigoryan[62], B. Grinyov[3], N. Grion[106], J. F. Grosse-Oetringhaus[34], J.-Y. Grossiord[124], R. Grosso[34], F. Guber[52], R. Guernane[67], B. Guerzoni[26], M. Guilbaud[124], K. Gulbrandsen[76], H. Gulkanyan[1], M. Gumbo[85], T. Gunji[121], A. Gupta[86], R. Gupta[86], K. H. Khan[15], R. Haake[50], Ø. Haaland[17], C. Hadjidakis[47], M. Haiduc[58], H. Hamagaki[121], G. Hamar[130], L. D. Hanratty[98], A. Hansen[76], J. W. Harris[131], H. Hartmann[39], A. Harton[13], D. Hatzifotiadou[101], S. Hayashi[121], S. T. Heckel[49], M. Heide[50], H. Helstrup[35], A. Herghelegiu[74], G. Herrera Corral[11], B. A. Hess[33], K. F. Hetland[35], B. Hippolyte[51], J. Hladky[56], P. Hristov[34], M. Huang[17], T. J. Humanic[19], N. Hussain[41], T. Hussain[18], D. Hutter[39], D. S. Hwang[20], R. Ilkaev[95], I. Ilkiv[73], M. Inaba[122], G. M. Innocenti[25], C. Ionita[34], M. Ippolitov[96], M. Irfan[18], M. Ivanov[93], V. Ivanov[81], A. Jachołkowski[27], P. M. Jacobs[70], C. Jahnke[115], H. J. Jang[64], M. A. Janik[128], P. H. S. Y. Jayarathna[117], C. Jena[28], S. Jena[117], R. T. Jimenez Bustamante[59], P. G. Jones[98], H. Jung[40], A. Jusko[98], V. Kadyshevskiy[62], P. Kalinak[55], A. Kalweit[34], J. Kamin[49], J. H. Kang[132], V. Kaplin[72], S. Kar[126], A. Karasu Uysal[65], O. Karavichev[52], T. Karavicheva[52], E. Karpechev[52], U. Kebschull[48], R. Keidel[133], D. L. D. Keijdener[53], M. Keil SVN[34], M. M. Khan[18,c], P. Khan[97], S. A. Khan[126], A. Khanzadeev[81], Y. Kharlov[108], B. Kileng[35], B. Kim[132], D. W. Kim[40,64], D. J.

Kim[118], J. S. Kim[40], M. Kim[40], M. Kim[132], S. Kim[20], T. Kim[132], S. Kirsch[39], I. Kisel[39], S. Kiselev[54], A. Kisiel[128], G. Kiss[130], J. L. Klay[6], J. Klein[89], C. Klein-Bösing[50], A. Kluge[34], M. L. Knichel[93], A. G. Knospe[113], C. Kobdaj[34,110], M. Kofarago[34], M. K. Köhler[93], T. Kollegger[39], A. Kolojvari[125], V. Kondratiev[125], N. Kondratyeva[72], A. Konevskikh[52], V. Kovalenko[125], M. Kowalski[112], S. Kox[67], G. Koyithatta Meethaleveedu[44], J. Kral[118], I. Králik[55], A. Kravčáková[38], M. Krelina[37], M. Kretz[39], M. Krivda[55,98], F. Krizek[79], E. Kryshen[34], M. Krzewicki[39,93], V. Kučera[79], Y. Kucheriaev[96,a], T. Kugathasan[34], C. Kuhn[51], P. G. Kuijer[77], I. Kulakov[49], J. Kumar[44], P. Kurashvili[73], A. Kurepin[52], A. B. Kurepin[52], A. Kuryakin[95], S. Kushpil[79], M. J. Kweon[46,89], Y. Kwon[132], P. Ladron de Guevara[59], C. Lagana Fernandes[115], I. Lakomov[47], R. Langoy[127], C. Lara[48], A. Lardeux[109], A. Lattuca[25], S. L. La Pointe[107], P. La Rocca[27], R. Lea[24], L. Leardini[89], G. R. Lee[98], I. Legrand[34], J. Lehnert[49], R. C. Lemmon[78], V. Lenti[100], E. Leogrande[53], M. Leoncino[25], I. León Monzón[114], P. Lévai[130], S. Li[7,66], J. Lien[127], R. Lietava[98], S. Lindal[21], V. Lindenstruth[39], C. Lippmann[93], M. A. Lisa[19], H. M. Ljunggren[32], D. F. Lodato[53], P. I. Loenne[17], V. R. Loggins[129], V. Loginov[72], D. Lohner[89], C. Loizides[70], X. Lopez[66], E. López Torres[9], X.-G. Lu[89], P. Luettig[49], M. Lunardon[28], G. Luparello[24,53], R. Ma[131], A. Maevskaya[52], M. Mager[34], D. P. Mahapatra[57], S. M. Mahmood[21], A. Maire[51,89], R. D. Majka[131], M. Malaev[81], I. Maldonado Cervantes[59], L. Malinina[62,d], D. Mal'Kevich[54], P. Malzacher[93], A. Mamonov[95], L. Manceau[107], V. Manko[96], F. Manso[66], V. Manzari[100], M. Marchisone[25,66], J. Mareš[56], G. V. Margagliotti[24], A. Margotti[101], A. Marín[93], C. Markert[34,113], M. Marquard[49], I. Martashvili[120], N. A. Martin[93], P. Martinengo[34], M. I. Martínez[2], G. Martínez García[109], J. Martin Blanco[109], Y. Martynov[3], A. Mas[109], S. Masciocchi[93], M. Masera[25], A. Masoni[102], L. Massacrier[109], A. Mastroserio[31], A. Matyja[112], C. Mayer[112], J. Mazer[120], M. A. Mazzoni[105], D. Mcdonald[117], F. Meddi[22], A. Menchaca-Rocha[60], E. Meninno[29], J. Mercado Pérez[89], M. Meres[36], Y. Miake[122], K. Mikhaylov[54,62], L. Milano[34], J. Milosevic[21,e], A. Mischke[53], A. N. Mishra[45], D. Miśkowiec[93], J. Mitra[126], C. M. Mitu[58], J. Mlynarz[129], N. Mohammadi[53], B. Mohanty[75,126], L. Molnar[51], L. Montaño Zetina[11], E. Montes[10], M. Morando[28], D. A. Moreira De Godoy[109,115], S. Moretto[28], A. Morreale[109], A. Morsch[34], V. Muccifora[68], E. Mudnic[111], D. Mühlheim[50], S. Muhuri[126], M. Mukherjee[126], H. Müller[34], M. G. Munhoz[115], S. Murray[85], L. Musa[34], J. Musinsky[55], B. K. Nandi[44], R. Nania[101], E. Nappi[100], C. Nattrass[120], K. Nayak[75], T. K. Nayak[126], S. Nazarenko[95], A. Nedosekin[54], M. Nicassio[93], M. Niculescu[34,58], J. Niedziela[34], B. S. Nielsen[76], S. Nikolaev[96], S. Nikulin[96], V. Nikulin[81], B. S. Nilsen[82], F. Noferini[12,101], P. Nomokonov[62], G. Nooren[53], J. Norman[119], A. Nyanin[96], J. Nystrand[17], H. Oeschler[89], S. Oh[131], S. K. Oh[40,63,f], A. Okatan[65], L. Olah[130], J. Oleniacz[128], A. C. Oliveira Da Silva[115], J. Onderwaater[93], C. Oppedisano[107], A. Ortiz Velasquez[32,59], A. Oskarsson[32], J. Otwinowski[93,112], K. Oyama[89], M. Ozdemir[49], P. Sahoo[45], Y. Pachmayer[89], M. Pachr[37], P. Pagano[29], G. Paić[59], C. Pajares[16], S. K. Pal[126], A. Palmeri[103], D. Pant[44], V. Papikyan[1], G. S. Pappalardo[103], P. Pareek[45], W. J. Park[93], S. Parmar[83], A. Passfeld[50], D. I. Patalakha[108], V. Paticchio[100], B. Paul[97], T. Pawlak[128], T. Peitzmann[53], H. Pereira Da Costa[14], E. Pereira De Oliveira Filho[115], D. Peresunko[96], C. E. Pérez Lara[77], A. Pesci[101], V. Peskov[49], Y. Pestov[5], V. Petráček[37], M. Petran[37], M. Petris[74], M. Petrovici[74], C. Petta[27], S. Piano[106], M. Pikna[36], P. Pillot[109], O. Pinazza[34,101], L. Pinsky[117], D. B. Piyarathna[117], M. Płoskoń[70], M. Planinic[94,123], J. Pluta[128], S. Pochybova[130], P. L. M. Podesta-Lerma[114], M. G. Poghosyan[34,82], E. H. O. Pohjoisaho[42], B. Polichtchouk[108], N. Poljak[94,123], A. Pop[74], S. Porteboeuf-Houssais[66], J. Porter[70], B. Potukuchi[86], S. K. Prasad[4,129], R. Preghenella[12,101], F. Prino[107], C. A. Pruneau[129], I. Pshenichnov[52], M. Puccio[107], G. Puddu[23], P. Pujahari[129], V. Punin[95], J. Putschke[129], H. Qvigstad[21], A. Rachevski[106], S. Raha[4], S. Rajput[86], J. Rak[118], A. Rakotozafindrabe[14], L. Ramello[30], R. Raniwala[87], S. Raniwala[87], S. S. Räsänen[42], B. T. Rascanu[49], D. Rathee[81], A. W. Rauf[15], V. Razazi[23], K. F. Read[120], J. S. Real[67], K. Redlich[73,g], R. J. Reed[129,131], A. Rehman[17], P. Reichelt[49], M. Reicher[53], F. Reidt[34,89], R. Renfordt[49], A. R. Reolon[68], A. Reshetin[52], F. Rettig[39], J.-P. Revol[34], K. Reygers[89], V. Riabov[81], R. A. Ricci[69], T. Richert[32], M. Richter[21], P. Riedler[34], W. Riegler[34], F. Riggi[27], A. Rivetti[107], E. Rocco[53], M. Rodríguez Cahuantzi[2], A. Rodriguez Manso[77], K. Røed[21], E. Rogochaya[62], S. Rohni[86], D. Rohr[39], D. Röhrich[17], R. Romita[78,119], F. Ronchetti[68], L. Ronflette[109], P. Rosnet[66], A. Rossi[34], F. Roukoutakis[84], A. Roy[45], C. Roy[51], P. Roy[97], A. J. Rubio Montero[10], R. Rui[24], R. Russo[25], E. Ryabinkin[96], Y. Ryabov[81], A. Rybicki[112], S. Sadovsky[108], K. Šafařík[34], B. Sahlmuller[49], R. Sahoo[45], P. K. Sahu[57], J. Saini[126], S. Sakai[68], C. A. Salgado[16], J. Salzwedel[19], S. Sambyal[86], V. Samsonov[81], X. Sanchez Castro[51], F. J. Sánchez Rodríguez[114], L. Šándor[55], A. Sandoval[60], M. Sano[122], G. Santagati[27], D. Sarkar[126], E. Scapparone[101], F. Scarlassara[28], R. P. Scharenberg[91], C. Schiaua[74], R. Schicker[89], C. Schmidt[93], H. R. Schmidt[33], S. Schuchmann[49], J. Schukraft[34], M. Schulc[37], T. Schuster[131], Y. Schutz[34,109], K. Schwarz[93], K. Schweda[93], G. Scioli[26], E. Scomparin[107], R. Scott[120], G. Segato[28], J. E. Seger[82], Y. Sekiguchi[121], I. Selyuzhenkov[93], K. Senosi[61], J. Seo[92], E. Serradilla[10,60], A. Sevcenco[58], A. Shabetai[109], G. Shabratova[62], R. Shahoyan[34], A. Shangaraev[108], A. Sharma[86], N. Sharma[120], S. Sharma[86], K. Shigaki[43], K. Shtejer[9,25], Y. Sibiriak[96], S. Siddhanta[102], T. Siemiarczuk[73], D. Silvermyr[80], C. Silvestre[67], G. Simatovic[123], R. Singaraju[126], R. Singh[86], S. Singha[75,126], V. Singhal[126], B. C. Sinha[126], T. Sinha[97], B. Sitar[36], M. Sitta[30], T. B. Skaali[21], K. Skjerdal[17], M. Slupecki[118], N. Smirnov[131], R. J. M. Snellings[53], C. Søgaard[32], R. Soltz[71], J. Song[92], M. Song[132], F. Soramel[28], S. Sorensen[120], M. Spacek[37], E. Spiriti[68], I. Sputowska[112], M. Spyropoulou-Stassinaki[84], B. K. Srivastava[91], J. Stachel[89], I. Stan[58], G. Stefanek[73], M. Steinpreis[19], E. Stenlund[32], G. Steyn[61], J. H. Stiller[89], D. Stocco[109], M. Stolpovskiy[108], P. Strmen[36], A. A. P. Suaide[115], T. Sugitate[43], C. Suire[47], M. Suleymanov[15], R. Sultanov[54], M.

Šumbera[79], T. J. M. Symons[70], A. Szabo[36], A. Szanto de Toledo[115], I. Szarka[36], A. Szczepankiewicz[34], M. Szymanski[128], J. Takahashi[116], M. A. Tangaro[31], J. D. Tapia Takaki[47,h], A. Tarantola Peloni[49], A. Tarazona Martinez[34], M. Tariq[18], M. G. Tarzila[74], A. Tauro[34], G. Tejeda Muñoz[2], A. Telesca[34], K. Terasaki[121], C. Terrevoli[23], J. Thäder[93], D. Thomas[53], R. Tieulent[124], A. R. Timmins[117], A. Toia[49,104], V. Trubnikov[3], W. H. Trzaska[118], T. Tsuji[121], A. Tumkin[95], R. Turrisi[104], T. S. Tveter[21], K. Ullaland[17], A. Uras[124], G. L. Usai[23], M. Vajzer[79], M. Vala[55,62], L. Valencia Palomo[66], S. Vallero[25,89], P. Vande Vyvre[34], J. Van Der Maarel[53], J. W. Van Hoorne[34], M. van Leeuwen[53], A. Vargas[2], M. Vargyas[118], R. Varma[44], M. Vasileiou[84], A. Vasiliev[96], V. Vechernin[125], M. Veldhoen[53], A. Velure[17], M. Venaruzzo[24,69], E. Vercellin[25], S. Vergara Limón[2], R. Vernet[8], M. Verweij[129], L. Vickovic[111], G. Viesti[28], J. Viinikainen[118], Z. Vilakazi[61], O. Villalobos Baillie[98], A. Vinogradov[96], L. Vinogradov[125], Y. Vinogradov[95], T. Virgili[29], V. Vislavicius[32], Y. P. Viyogi[126], A. Vodopyanov[62], M. A. Völkl[89], K. Voloshin[54], S. A. Voloshin[129], G. Volpe[34], B. von Haller[34], I. Vorobyev[125], D. Vranic[34,93], J. Vrláková[38], B. Vulpescu[66], A. Vyushin[95], B. Wagner[17], J. Wagner[93], V. Wagner[37], M. Wang[7,109], Y. Wang[89], D. Watanabe[122], M. Weber[34,117], S. G. Weber[93], J. P. Wessels[50], U. Westerhoff[50], J. Wiechula[33], J. Wikne[21], M. Wilde[50], G. Wilk[73], J. Wilkinson[89], M. C. S. Williams[101], B. Windelband[89], M. Winn[89], C. G. Yaldo[129], Y. Yamaguchi[121], H. Yang[53], P. Yang[7], S. Yang[17], S. Yano[43], S. Yasnopolskiy[96], J. Yi[92], Z. Yin[7], I.-K. Yoo[92], I. Yushmanov[96], V. Zaccolo[76], C. Zach[37], A. Zaman[15], C. Zampolli[101], S. Zaporozhets[62], A. Zarochentsev[125], P. Závada[56], N. Zaviyalov[95], H. Zbroszczyk[128], I. S. Zgura[58], M. Zhalov[81], H. Zhang[7], X. Zhang[7,70], Y. Zhang[7], C. Zhao[21], N. Zhigareva[54], D. Zhou[7], F. Zhou[7], Y. Zhou[53], Zhou Zhuo[17], H. Zhu[7], J. Zhu[7,109], X. Zhu[7], A. Zichichi[12,26], A. Zimmermann[89], M. B. Zimmermann[34,50], G. Zinovjev[3], Y. Zoccarato[124], M. Zyzak[49]

[1] A.I. Alikhanyan National Science Laboratory (Yerevan Physics Institute) Foundation, Yerevan, Armenia
[2] Benemérita Universidad Autónoma de Puebla, Puebla, Mexico
[3] Bogolyubov Institute for Theoretical Physics, Kiev, Ukraine
[4] Department of Physics and Centre for Astroparticle Physics and Space Science (CAPSS), Bose Institute, Kolkata, India
[5] Budker Institute for Nuclear Physics, Novosibirsk, Russia
[6] California Polytechnic State University, San Luis Obispo, CA, USA
[7] Central China Normal University, Wuhan, China
[8] Centre de Calcul de l'IN2P3, Villeurbanne, France
[9] Centro de Aplicaciones Tecnológicas y Desarrollo Nuclear (CEADEN), Havana, Cuba
[10] Centro de Investigaciones Energéticas Medioambientales y Tecnológicas (CIEMAT), Madrid, Spain
[11] Centro de Investigación y de Estudios Avanzados (CINVESTAV), Mexico City and Mérida, Mexico
[12] Centro Fermi-Museo Storico della Fisica e Centro Studi e Ricerche "Enrico Fermi", Rome, Italy
[13] Chicago State University, Chicago, USA
[14] Commissariat à l'Energie Atomique, IRFU, Saclay, France
[15] COMSATS Institute of Information Technology (CIIT), Islamabad, Pakistan
[16] Departamento de Física de Partículas and IGFAE, Universidad de Santiago de Compostela, Santiago de Compostela, Spain
[17] Department of Physics and Technology, University of Bergen, Bergen, Norway
[18] Department of Physics, Aligarh Muslim University, Aligarh, India
[19] Department of Physics, Ohio State University, Columbus, OH, USA
[20] Department of Physics, Sejong University, Seoul, South Korea
[21] Department of Physics, University of Oslo, Oslo, Norway
[22] Dipartimento di Fisica dell'Università 'La Sapienza' and Sezione INFN, Rome, Italy
[23] Dipartimento di Fisica dell'Università and Sezione INFN, Cagliari, Italy
[24] Dipartimento di Fisica dell'Università and Sezione INFN, Trieste, Italy
[25] Dipartimento di Fisica dell'Università and Sezione INFN, Turin, Italy
[26] Dipartimento di Fisica e Astronomia dell'Università and Sezione INFN, Bologna, Italy
[27] Dipartimento di Fisica e Astronomia dell'Università and Sezione INFN, Catania, Italy
[28] Dipartimento di Fisica e Astronomia dell'Università and Sezione INFN, Padua, Italy
[29] Dipartimento di Fisica 'E.R. Caianiello' dell'Università and Gruppo Collegato INFN, Salerno, Italy
[30] Dipartimento di Scienze e Innovazione Tecnologica dell'Università del Piemonte Orientale and Gruppo Collegato INFN, Alessandria, Italy
[31] Dipartimento Interateneo di Fisica 'M. Merlin' and Sezione INFN, Bari, Italy
[32] Division of Experimental High Energy Physics, University of Lund, Lund, Sweden
[33] Eberhard Karls Universität Tübingen, Tübingen, Germany

[34] European Organization for Nuclear Research (CERN), Geneva, Switzerland
[35] Faculty of Engineering, Bergen University College, Bergen, Norway
[36] Faculty of Mathematics, Physics and Informatics, Comenius University, Bratislava, Slovakia
[37] Faculty of Nuclear Sciences and Physical Engineering, Czech Technical University in Prague, Prague, Czech Republic
[38] Faculty of Science, P.J. Šafárik University, Kosice, Slovakia
[39] Frankfurt Institute for Advanced Studies, Johann Wolfgang Goethe-Universität Frankfurt, Frankfurt, Germany
[40] Gangneung-Wonju National University, Gangneung, South Korea
[41] Department of Physics, Gauhati University, Guwahati, India
[42] Helsinki Institute of Physics (HIP), Helsinki, Finland
[43] Hiroshima University, Hiroshima, Japan
[44] Indian Institute of Technology Bombay (IIT), Mumbai, India
[45] Indian Institute of Technology Indore (IITI), Indore, India
[46] Inha University, Inchon, South Korea
[47] Institut de Physique Nucléaire d'Orsay (IPNO), Université Paris-Sud, CNRS-IN2P3, Orsay, France
[48] Institut für Informatik, Johann Wolfgang Goethe-Universität Frankfurt, Frankfurt, Germany
[49] Institut für Kernphysik, Johann Wolfgang Goethe-Universität Frankfurt, Frankfurt, Germany
[50] Institut für Kernphysik, Westfälische Wilhelms-Universität Münster, Münster, Germany
[51] Institut Pluridisciplinaire Hubert Curien (IPHC), Université de Strasbourg, CNRS-IN2P3, Strasbourg, France
[52] Institute for Nuclear Research, Academy of Sciences, Moscow, Russia
[53] Institute for Subatomic Physics of Utrecht University, Utrecht, The Netherlands
[54] Institute for Theoretical and Experimental Physics, Moscow, Russia
[55] Institute of Experimental Physics, Slovak Academy of Sciences, Kosice, Slovakia
[56] Institute of Physics, Academy of Sciences of the Czech Republic, Prague, Czech Republic
[57] Institute of Physics, Bhubaneswar, India
[58] Institute of Space Science (ISS), Bucharest, Romania
[59] Instituto de Ciencias Nucleares, Universidad Nacional Autónoma de México, Mexico City, Mexico
[60] Instituto de Física, Universidad Nacional Autónoma de México, Mexico City, Mexico
[61] iThemba LABS, National Research Foundation, Somerset West, South Africa
[62] Joint Institute for Nuclear Research (JINR), Dubna, Russia
[63] Konkuk University, Seoul, South Korea
[64] Korea Institute of Science and Technology Information, Taejeon, South Korea
[65] KTO Karatay University, Konya, Turkey
[66] Laboratoire de Physique Corpusculaire (LPC), Clermont Université, Université Blaise Pascal, CNRS-IN2P3, Clermont-Ferrand, France
[67] Laboratoire de Physique Subatomique et de Cosmologie, Université Grenoble-Alpes, CNRS-IN2P3, Grenoble, France
[68] Laboratori Nazionali di Frascati, INFN, Frascati, Italy
[69] Laboratori Nazionali di Legnaro, INFN, Legnaro, Italy
[70] Lawrence Berkeley National Laboratory, Berkeley, CA, USA
[71] Lawrence Livermore National Laboratory, Livermore, CA, USA
[72] Moscow Engineering Physics Institute, Moscow, Russia
[73] National Centre for Nuclear Studies, Warsaw, Poland
[74] National Institute for Physics and Nuclear Engineering, Bucharest, Romania
[75] National Institute of Science Education and Research, Bhubaneswar, India
[76] Niels Bohr Institute, University of Copenhagen, Copenhagen, Denmark
[77] Nikhef, National Institute for Subatomic Physics, Amsterdam, The Netherlands
[78] Nuclear Physics Group, STFC Daresbury Laboratory, Daresbury, UK
[79] Nuclear Physics Institute, Academy of Sciences of the Czech Republic, Řež u Prahy, Czech Republic
[80] Oak Ridge National Laboratory, Oak Ridge, TN, USA
[81] Petersburg Nuclear Physics Institute, Gatchina, Russia
[82] Physics Department, Creighton University, Omaha, NE, USA
[83] Physics Department, Panjab University, Chandigarh, India
[84] Physics Department, University of Athens, Athens, Greece
[85] Physics Department, University of Cape Town, Cape Town, South Africa

[86] Physics Department, University of Jammu, Jammu, India
[87] Physics Department, University of Rajasthan, Jaipur, India
[88] Physik Department, Technische Universität München, Munich, Germany
[89] Physikalisches Institut, Ruprecht-Karls-Universität Heidelberg, Heidelberg, Germany
[90] Politecnico di Torino, Turin, Italy
[91] Purdue University, West Lafayette, IN, USA
[92] Pusan National University, Pusan, South Korea
[93] Research Division and ExtreMe Matter Institute EMMI, GSI Helmholtzzentrum für Schwerionenforschung, Darmstadt, Germany
[94] Rudjer Bošković Institute, Zagreb, Croatia
[95] Russian Federal Nuclear Center (VNIIEF), Sarov, Russia
[96] Russian Research Centre Kurchatov Institute, Moscow, Russia
[97] Saha Institute of Nuclear Physics, Kolkata, India
[98] School of Physics and Astronomy, University of Birmingham, Birmingham, UK
[99] Sección Física, Departamento de Ciencias, Pontificia Universidad Católica del Perú, Lima, Peru
[100] Sezione INFN, Bari, Italy
[101] Sezione INFN, Bologna, Italy
[102] Sezione INFN, Cagliari, Italy
[103] Sezione INFN, Catania, Italy
[104] Sezione INFN, Padua, Italy
[105] Sezione INFN, Rome, Italy
[106] Sezione INFN, Trieste, Italy
[107] Sezione INFN, Turin, Italy
[108] SSC IHEP of NRC Kurchatov institute, Protvino, Russia
[109] SUBATECH, Ecole des Mines de Nantes, Université de Nantes, CNRS-IN2P3, Nantes, France
[110] Suranaree University of Technology, Nakhon Ratchasima, Thailand
[111] Technical University of Split FESB, Split, Croatia
[112] The Henryk Niewodniczanski Institute of Nuclear Physics, Polish Academy of Sciences, Kracòw, Poland
[113] Physics Department, The University of Texas at Austin, Austin, TX, USA
[114] Universidad Autónoma de Sinaloa, Culiacán, Mexico
[115] Universidade de São Paulo (USP), São Paulo, Brazil
[116] Universidade Estadual de Campinas (UNICAMP), Campinas, Brazil
[117] University of Houston, Houston, TX, USA
[118] University of Jyväskylä, Jyväskylä, Finland
[119] University of Liverpool, Liverpool, UK
[120] University of Tennessee, Knoxville, TN, USA
[121] University of Tokyo, Tokyo, Japan
[122] University of Tsukuba, Tsukuba, Japan
[123] University of Zagreb, Zagreb, Croatia
[124] Université de Lyon, Université Lyon 1, CNRS/IN2P3, IPN-Lyon, Villeurbanne, France
[125] V. Fock Institute for Physics, St. Petersburg State University, St. Petersburg, Russia
[126] Variable Energy Cyclotron Centre, Kolkata, India
[127] Vestfold University College, Tonsberg, Norway
[128] Warsaw University of Technology, Warsaw, Poland
[129] Wayne State University, Detroit, MI, USA
[130] Wigner Research Centre for Physics, Hungarian Academy of Sciences, Budapest, Hungary
[131] Yale University, New Haven, CT, USA
[132] Yonsei University, Seoul, South Korea
[133] Zentrum für Technologietransfer und Telekommunikation (ZTT), Fachhochschule Worms, Worms, Germany

[a] Deceased
[b] Also at: St. Petersburg State Polytechnical, St. Petersburg, Russia, University
[c] Also at: Department of Applied Physics, Aligarh Muslim University, Aligarh, India

[d] Also at: M.V. Lomonosov Moscow State University, D.V. Skobeltsyn Institute of Nuclear Physics, Moscow, Russia
[e] Also at: University of Belgrade, Faculty of Physics and "Vinča" Institute of Nuclear Sciences, Belgrade, Serbia
[f] *Permanent Address*: Konkuk University, Seoul, Korea
[g] Also at: Institute of Theoretical Physics, University of Wroclaw, Wroclaw, Poland
[h] Also at: University of Kansas, Lawrence, KS, USA